INSTITUTE OF PHYSICS PUBLISHING JOURNAL OF PHYSICS B: ATOMIC, MOLECULAR AND OPTICAL PHYSICS

J. Phys. B: At. Mol. Opt. Phys. **38** (2005) 525–545 doi:10.1088/0953-4075/38/5/006

Semiempirical formulae for electron-impact double-ionization cross sections of light positive ions

V P Shevelko[1], H Tawara[2,3], F Scheuermann[4], B Fabian[4], A Müller[4] and E Salzborn[4]

[1] P N Lebedev Physical Institute, 119991 Moscow, Russia
[2] Max-Planck Institute for Nuclear Physics, D-69117 Heidelberg, Germany
[3] Department of Physics, The Queen's University, Belfast BT7 1NN, UK
[4] Institute for Atomic and Molecular Physics, D-35392 Giessen, Germany

E-mail: shev@sci.lebedev.ru

Received 21 October 2004
Published 21 February 2005
Online at stacks.iop.org/JPhysB/38/525

Abstract

Electron-impact double-ionization processes of light positive ions from He- to Ne-like isoelectronic sequences, as well as of the heavy ions Ar^{q+} ($q = 1$–7) and Kr^{q+} ($q = 1$–4) are considered for incident-electron energies $E < 50\,I_{th}$ where I_{th} is the threshold energy for double-electron ionization. On the basis of reliable experimental data and quantum-mechanical calculations, simple semiempirical formulae with three fitting parameters, by taking into account the contribution of direct double ionization and of inner-shell ionization processes, are obtained which describe the experimental cross sections within an accuracy of 20–30%. With this accuracy, the formulae suggested can be used for prediction of the double-ionization cross sections of positive ions with the nuclear charge $Z \leqslant 26$ in the electron energy range of $E < 50 I_{th}$. According to the model suggested, the direct ionization cross section σ_{dir} (simultaneous ionization of two outer electrons) is scaled as I_{th}^{-3} against scaled electron energy E/I_{th} and contains only one fitting parameter. Two additional fitting parameters are obtained using the least-squares method in conjunction with numerically calculated single-electron inner-shell ionization cross sections. All fitting parameters are found to be constant for ions within a given isoelectronic sequence. The present analysis also provides a method for indirect determination of K-shell ionization cross sections for ions from Be-like to Ne-like sequences. The fluorescence yields ω_K for a single K-shell vacancy in ions from Li-like to Ne-like sequences with nuclear charges $3 \leqslant Z \leqslant 26$ are calculated as well.

 © 2005 IOP Publishing Ltd Printed in the UK

1. Introduction

Presently, a large amount of experimental data on electron-impact multi-electron ionization cross sections of atoms, and of negative and positive ions is available (see, e.g., Tawara and Kato 1987, Shevelko and Tawara 1998, Tawara and Kato 1999). Single- and double-ionization, as well as multiple ionization of positive ions, are of special interest because these processes play a dominant role in almost all laboratory and astrophysical plasma sources. Whereas quite accurate calculations of single-electron ionization cross sections can be performed by several numerical methods, the multi-electron processes still need to be interpreted in terms of increasingly sophisticated treatments. Furthermore, theoretical difficulties arise very rapidly with the increasing number of ejected electrons, and, therefore, semiempirical formulae are often used to estimate multi-electron ionization cross sections.

In heavy low-charged multi-electron ion targets, many subshells and many direct and indirect processes can contribute to the total double-ionization processes, making the corresponding cross sections a relatively smooth function of the incident electron energy. In this case, the cross sections can be estimated in general by existing semiempirical formulae (Fisher *et al* 1995, Bélenger *et al* 1997) within a factor of 2.

Experimental double-ionization cross sections of light ions (with the nuclear charge $Z \leqslant 18$) show a well-distinguished two-maximum structure: the first maximum is due to simultaneous ionization of two of the outer-most electrons, and the second one is caused by the 1s-inner-shell ionization followed by subsequent autoionization. For light atoms and ions, the known semiempirical formulae (see, e.g., Zambra *et al* 1994, Fisher *et al* 1995, Deutsch *et al* 1996, Bélenger *et al* 1997) can describe the double-ionization cross sections on average but not the two-maximum structure. Moreover, these formulae can lead to a discrepancy of up to a factor of 10 and, therefore, cannot provide a proper description of the experimental data.

In order to obtain simple and reliable semiempirical formulae for double-ionization of light ions, the existing experimental data for ions from He-like to Ne-like isoelectronic sequences were surveyed and analysed. The data were obtained mainly by two experimental groups: in Belgium (Université Catholique de Louvain) and Germany (University of Giessen). We believe that a more consistent set of data was obtained in Giessen at the electron-ion crossed-beam set-up described in detail in Tinschert *et al* (1989) and Hofmann *et al* (1990). There, the dynamic crossed-beam technique was employed (Müller *et al* 1985a, 1985b) where the electron gun and, thus, the electron beam were moved mechanically up and down across the ion beam at a fixed position with simultaneous registration of the ionization signal of ions, the electron and the ion currents. The total experimental uncertainties of the measured cross sections are typically 8% at the maximum resulting from the non-statistical errors of about 7.8% and the statistical error at 95% confidence level.

In the present work, on the basis of the experimental data and quantum-mechanical calculations, new semiempirical formulae are obtained for the double-ionization cross sections of light ions which describe the experimental data with an accuracy of about 20–30% including the two-maximum structure. The procedure for obtaining these formulae as well as a comparison with the experimental data are given together with the fitting parameters, binding and threshold energies and branching ratios for a single 1s-shell vacancy. It is shown that the method suggested can also be applied to heavier targets such as argon and krypton ions, providing a good agreement with the observed results.

2. Theoretical model for electron-impact double-ionization cross sections

The direct and indirect processes leading to the creation of two additional 'free' electrons (so-called double ionization)

$$e^- + X^{q+} \rightarrow X^{(q+2)+} + 3\,e^- \tag{1}$$

have been already discussed in many papers (see, e.g., Andersen *et al* (1987); Müller (1991, 2002); McGuire (1992)). Here X^{q+} denotes a target atom/ion with the charge q. Briefly, the following three main processes are responsible for reaction (1):

(i) direct ionization of two of the outermost electrons,
(ii) indirect processes related to ionization (or excitation) of a single inner-shell electron of the target followed by Auger decay(s),
(iii) resonant excitation–triple-autoionization consisting of the capture of the incident electron by the target ion into a highly excited state which decays by sequential or simultaneous emission of three electrons.

For the ionization of light ions, processes (i) and (ii) are the most important ones, while for complex many-electron, highly charged ions all processes, particularly process (iii), become important and should be taken into account (see, e.g., Müller 1991).

The double-ionization cross section σ_2 for relatively light target ions can be represented in the adopted form (see, e.g., Andersen *et al* 1987):

$$\sigma_2 = \sigma_{\rm dir} + \sigma_{\rm indir} \equiv \sigma_{\rm dir} + \sum_{\gamma} a_\gamma \sigma_\gamma, \qquad I_\gamma \geqslant I_{\rm th}, \tag{2}$$

where $\sigma_{\rm dir}$ denotes the *direct* double-ionization cross section describing simultaneous ionization of two of the outermost electrons (i), and the second term, $\sigma_{\rm indir}$, comprises *indirect* processes related to single ionization from inner shells followed by autoionization (ii). Here, $I_{\rm th}$ denotes the threshold energy for double ionization. Usually, it is the sum of the first (I_1) and the second (I_2) ionization potential of the target ion X^{q+}:

$$I_{\rm th} = I_1 + I_2, \tag{3}$$

which coincides with experimental values in most cases. σ_γ is the electron-impact single-ionization cross section of the inner-shell γ, and a_γ is the corresponding branching ratio for autoionization processes given by

$$a_\gamma = \frac{A_{\rm a}^{(\gamma)}}{A_{\rm a}^{(\gamma)} + A_{\rm r}^{(\gamma)}}. \tag{4}$$

Here $A_{\rm a}^{(\gamma)}$ and $A_{\rm r}^{(\gamma)}$ denote the autoionization and radiative decay rates, respectively, for the ion $X^{(q+1)+}$ having a vacancy in the shell γ. We note that the summation over γ in (2) has to be restricted to those inner-shell electrons for which their binding energy I_γ is equal to or larger than the threshold energy, i.e., $I_\gamma \geqslant I_{\rm th}$.

When we consider the double ionization of light ions with $Z < 14$, the autoionization decay rates by far dominate the radiative decay rates and, thus, the parameter a_γ is very close to unity for most of these ions. For Li-like to Ne-like ions with $3 \leqslant Z \leqslant 26$, the K-shell fluorescence yields $\omega_{\rm K} = 1 - a_{1s}$ are calculated in section 4.

2.1. Analysis of the direct part σ_{dir}

From the analysis of the available experimental data for direct double-ionization cross sections $\sigma_{\rm dir}$ of ions, the following dependences can be found:

(i) Cross sections $\sigma_{\rm dir}$ reach their maximum at the electron energy of $E_{\rm dir}^{\rm max} \approx 2.5\, I_{\rm th}$.
(ii) Maximum direct-ionization cross sections $\sigma_{\rm dir}^{\rm max}$ are proportional to $I_{\rm th}^{-3}$.

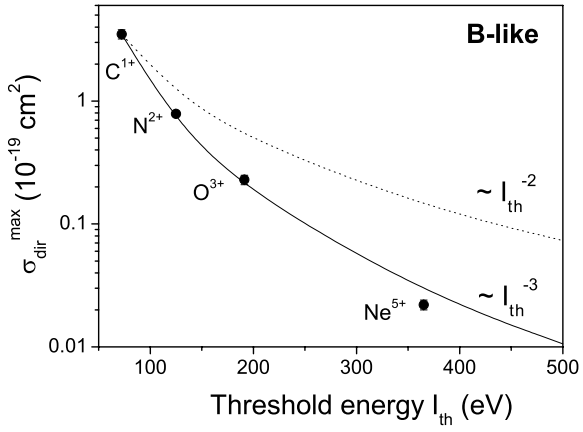

Figure 1. Dependence of $\sigma_{\rm dir}^{\rm max}$ values for ionization of B-like ions as a function of the threshold energy $I_{\rm th}$. Solid circles: experimental data for C^{1+}, N^{2+}, O^{3+} (Westermann *et al* 1999), and Ne^{5+} (Duponchelle *et al* 1997). Note that the solid line fits the experimental data with their $I_{\rm th}^{-3}$ dependence, while the dotted line shows the usual $I_{\rm th}^{-2}$ dependence, for comparison.

Using these properties, one can describe the direct part of the double-ionization cross section by a model cross section in the empirical form:

$$\sigma_{\rm dir}(E) = 10^{-13}\,{\rm cm}^2(1-{\rm e}^{-3(u-1)})\frac{A_{\rm dir}}{I_{\rm th}^3}\frac{u-1}{(u+0.5)^2}, \qquad u = E/I_{\rm th}, \tag{5}$$

where $A_{\rm dir}$ is the fitting parameter (in eV^3 units), and u the scaled energy of the incident electron and $I_{\rm th}$ is given in eV. The factor $(1-{\rm e}^{-3(u-1)})$ is introduced to provide the correct asymptotic behaviour (Wannier (1953) law) of $\sigma_{\rm dir}(E)$ for the double ionization in the vicinity of the threshold: $\sigma_{\rm dir}\,(E) \sim (E-I_{\rm th})^2$ at $E \sim I_{\rm th}$.

The cross section (5) has the following asymptotic behaviour:

$$\sigma_{\rm dir}(E) \sim \begin{cases} (E-I_{\rm th})^2, & E \to I_{\rm th}, \\ A_{\rm dir}\big/\big(EI_{\rm th}^2\big), & E \gg I_{\rm th}, \end{cases} \tag{6}$$

and $\sigma_{\rm dir}^{\rm max} \sim I_{\rm th}^{-3}$ at an energy of $E_{\rm dir}^{\rm max} \approx 2.5I_{\rm th}$. These properties can be compared with the classical single-ionization cross-section behaviour: $\sigma_1 \sim 1/(EI_{\rm th})$ at $E \gg I_{\rm th}$ and $\sigma_1^{\rm max} \sim I_{\rm th}^{-2}$ at $E_1^{\rm max} \approx 2I_{\rm th}$.

The choice of $\sigma_{\rm dir}$ in the form (5) can be justified by several arguments. First of all, as was already mentioned, the property $\sigma_{\rm dir}^{\rm max} \sim I_{\rm th}^{-3}$ is suggested by the available experimental data. For B-like ions figure 1 shows a typical dependence of $\sigma_{\rm dir}^{\rm max}$ on the threshold energy $I_{\rm th}$. Obviously, experimental values are well represented by the $I_{\rm th}^{-3}$ law instead of the expected $I_{\rm th}^{-2}$-dependence valid for electron-impact single-ionization cross sections.

Secondly, the asymptotic dependence $\sigma_{\rm dir} \sim 1\big/\big(EI_{\rm th}^2\big)$ at $E \gg I_{\rm th}$, shown in equation (6), also follows from the behaviour of the direct double-ionization cross sections of He-like ions by electrons considered by Bélenger *et al* (1997). There, using a scaling law for the double-photoionization cross sections, the following asymptotic form for $\sigma_{\rm dir}$ was obtained:

$$\sigma_{\rm dir}(E) \approx \frac{A}{E}\ln(BE) + \frac{C}{E} + \frac{D}{E^2} + \cdots, \qquad E \gg I_{\rm th}, \tag{7}$$

where A, B, C and D are constants depending on the nuclear charge Z of the target ion. Comparing the $1/C$ values in equation (7) with the threshold energies $I_{\rm th} = I_1 + I_2$ as a

function of the nuclear charge Z for He-like ions, and using the I_1 and I_2 values from the tables (*Handbook of Chemistry and Physics* 2001), one can easily find that $C \sim I_{\rm th}^{-2}$, i.e., similar to the high-energy term in equation (6).

In this paper, we assume that physical mechanisms leading to simultaneous ionization of two target electrons in He-like ions are similar to the ions considered, and therefore, the scaling for ions from other isoelectronic sequences is also similar. Some additional arguments for using the model cross section (5) are considered in section 3.4.

2.2. Cross sections for single-electron ionization of inner shells

Calculation of the cross sections for single inner-shell ionization in equation (2) is not a big issue and it can easily be done using, e.g., the CBE approximation (Coulomb–Born with exchange) or the DW approximation (distorted wave). In this work, the σ_γ values were calculated in the CBE approximation using the ATOM code (see Shevelko and Vainshtein (1993)) and fitted in the form:

$$\sigma_\gamma(E) = 10^{-13}\,\mathrm{cm}^2 \frac{C_\gamma}{I_\gamma^2}\frac{x-1}{x(x+\varphi_\gamma)}, \qquad x = E/I_\gamma \geqslant 1, \tag{8}$$

where I_γ is the binding energy of an electron in the inner-shell γ (in eV), and x is the incident-electron energy scaled to I_γ. Here C_γ (in eV^2) and φ_γ are the fitting parameters which are found by the least-squares method (LSM) from numerical calculations. The cross section in equation (8) has the following asymptotic behaviour:

$$\sigma_\gamma(E) \sim \begin{cases} (E - I_\gamma), & E \to I_\gamma, \\ C_\gamma/(EI_\gamma), & E \gg I_\gamma. \end{cases} \tag{9}$$

The cross section at its maximum is inversely proportional to I_γ^2, i.e., $\sigma_\gamma^{\max} \sim I_\gamma^{-2}$ at an energy of $E_\gamma^{\max} \approx I_\gamma\sqrt{\varphi_\gamma}$.

Finally, the total double-ionization cross section σ_2 in (2) can be represented in the form

$$\sigma_2(E) = 10^{-13}\,\mathrm{cm}^2\left[(1 - \mathrm{e}^{-3(u-1)})\frac{A_{\rm dir}}{I_{\rm th}^3}\frac{u-1}{(u+0.5)^2} + \sum_\gamma a_\gamma \frac{C_\gamma}{I_\gamma^2}\frac{x-1}{x(x+\varphi_\gamma)}\right], \tag{10}$$

$$u = E/I_{\rm th} \geqslant 1, \qquad x = E/I_\gamma \geqslant 1, \tag{11}$$

where E denotes the incident electron energy, $I_{\rm th}$ the threshold energy of double ionization, I_γ the binding energy of the inner-shell electron (all energies in eV), and a_γ the branching ratio (4). Here $A_{\rm dir}$ (in eV^3), C_γ (in eV^2) and φ_γ (dimensionless) are the fitting parameters. Summation in equation (10) has to be carried out for all inner-shell electrons for which $I_\gamma \geqslant I_{\rm th}$; if $I_\gamma < I_{\rm th}$ then $C_\gamma = 0$.

Strictly speaking, both direct and indirect parts of the cross sections in (10) should contain the Bethe logarithmic terms which are important at high electron energies. However, we think that in the considered energy range of $E < 50I_{\rm th}$, the inclusion of the logarithmic parts in semiempirical formula (10) is not necessary because the fitting parameters are obtained with account for experimental cross sections available in this energy range and provide an accuracy of about 20–30% (see the next section). The condition $E < 50I_{\rm th}$ gives a limitation of using equation (10) on the electron energy E. Another limitation is put on the nuclear charge of the target ion Z: it should be not larger than about $Z \leqslant 26$. For heavier ions with $Z > 26$, one has to include the logarithmic terms and to calculate the fitting parameters with account for relativistic effects in the wavefunctions and the interaction potentials.

3. Numerical calculations and comparison with experiment

Calculations of the fitting parameters, $A_{\rm dir}$, C_γ and φ_γ, and, thus, total double-ionization cross sections (10) were made for He-, Li-, Be-, B-, C-, N-, O-, F- and Ne-like ions, for Ar^{q+} ions with $q = 1$–7 and also for Kr^{q+} ions with $q = 1$–4. The binding energies I_1 and I_2 were taken from the tables (*Handbook of Chemistry and Physics* 2001), and the inner-shell binding energies I_γ were calculated in the present work using the GRASP code described by Dyall *et al* (1989). The binding and threshold energies used in this work are given in tables 1 and 3.

The fitting parameters $A_{\rm dir}$ were found by comparing equation (5) with experimental data obtained mainly by the Giessen group. Single-electron inner-shell ionization cross sections σ_γ were calculated in the CBE approximation by the ATOM code using the partial-wave representation (see Shevelko and Vainshtein (1993) for details). The radial wavefunctions of the bound and ionized electrons were calculated by solving the radial Schrödinger equation with the central effective field of the atomic core, and for the incident and scattered electrons, Coulomb wavefunctions were used. The calculated relevant parameters, $A_{\rm dir}$, C_γ and φ_γ, are given in tables 2, 4 and 5.

We note that for ions from Be- to Ne-like isoelectronic sequences, the double-ionization cross sections have a simple form following equation (2):

$$\sigma_2 = \sigma_{\rm dir} + a_{1s}\sigma_{1s}, \qquad I_{1s} \geqslant I_{\rm th}. \tag{12}$$

In the following, we will discuss the most important features of double-ionization cross sections for the isoelectronic sequences mentioned.

3.1. He-like ions

It is well known that there are various mechanisms contributing to the double-ionization of He (McGuire 1992). In the present context those mechanisms are summarized as direct double-ionization of the two 1s electrons. The cross sections for direct double ionization of He-like atoms or ions show a single maximum. Scaled double-ionization cross sections for He-like systems are displayed in figure 2. The maximum of the scaled cross sections appears to be shifted towards higher energies, i.e., $E_{\rm dir}^{\rm max} \approx (3\text{–}4)I_{\rm th}$. Probably, this is related to the influence of strong correlation effects between two electrons in He-like systems.

3.2. Li-like ions

In these ions, we expect some interesting features because the binding energy I_{1s} of the inner-shell 1s electrons is naturally smaller than the threshold energy of double ionization $I_{\rm th}$, and the ejection of a single 1s-electron from the K-shell does not lead to autoionization, but could lead to shake-off. Thus, the direct double-ionization process by far dominates the production of two additional free electrons in the final channel. Indeed, the observed double-ionization cross sections of Li-like ions have only one maximum due to direct double-electron ionization, similar to He-like ions. So far, experimental data are known only for Li, C^{3+} and N^{4+} systems. A typical example for double ionization is given in figure 3 for C^{3+} ions.

3.3. Be-like ions

Experimental data for double ionization of Be-like ions have systematically been measured for B^+, C^{2+}, N^{3+}, O^{4+} and Ne^{6+} ions (Tinschert 1989, Westermann *et al* 1999, Scheuermann *et al* 2001). The cross sections for B^+ and C^{2+} ions have two pronounced maxima caused by both

Table 1. First (I_1), second (I_2) ionization potentials, threshold energies I_{th} and binding energies I_{1s} (all in eV). The values of I_1 and I_2 are taken from tables (*Handbook of Chemistry and Physics* 2001), I_{1s} were calculated by the GRASP code (Dyall *et al* 1989) except for He-like and Li-like ions for which the data were taken from *Handbook of Chemistry and Physics* (2001) and Lotz (1970) tables, respectively.

Sequence	I_1	I_2	$I_{th} = I_1 + I_2$	I_{1s}
		He-like		
He^{0+}	24.587	54.416	79.00	24.587
Li^{1+}	75.638	122.451	198.09	75.638
B^{3+}	259.368	340.217	599.59	259.368
C^{4+}	392.077	489.981	882.06	392.077
		Li-like		
Li^{0+}	5.392	75.638	81.03	58
C^{3+}	64.492	392.077	456.57	344
N^{4+}	97.888	552.057	649.95	494
		Be-like		
B^{1+}	25.154	37.930	63.084	217.66
C^{2+}	47.887	64.492	112.38	339.36
N^{3+}	77.472	97.888	175.36	487.37
O^{4+}	113.896	138.116	252.012	664.69
Ne^{6+}	207.27	239.09	446.36	1099.31
		B-like		
B^{0+}	8.298	25.154	33.452	200.33
C^{1+}	24.383	47.887	72.27	316.638
N^{2+}	47.448	77.472	124.92	459.09
O^{3+}	77.412	113.896	191.38	629.09
Ne^{5+}	157.93	207.27	365.2	1051.16
Fe^{21+}	1793.08	1943.61	3736.7	8404.06
		C-like ions		
N^{1+}	29.601	47.448	77.049	431.3
O^{2+}	54.934	77.412	132.346	595.59
		N-like		
O^{1+}	32.54	52.59	85.13	568.41
		O-like		
O^{0+}	13.618	35.116	48.734	544.33
Ne^{2+}	63.45	97.11	160.56	926.38
		F-like		
Ne^{1+}	40.962	63.65	104.612	896.79
Al^{4+}	153.71	190.47	344.18	1654.82
		Ne-like		
Al^{3+}	119.99	153.71	273.7	1607.92

the simultaneous ionization of two outer electrons and single ionization from the K-shell. As shown in figure 4, we reproduce the experimental cross section for B^{1+} ions quite well.

3.4. B-like ions

Double ionization of B-like ions turns out to be the most interesting case because the corresponding cross sections have two maxima of comparable magnitudes. Experimental

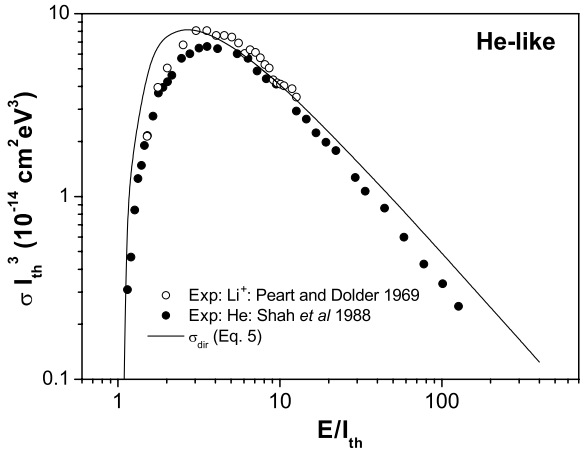

Figure 2. Scaled double-ionization cross sections of He-like ions. Symbols: experimental data: open circles, Li^+ (Peart and Dolder 1969); solid circles, He (Shah *et al* 1988). Solid curve: direct cross section (equation (5)).

Table 2. Fitting constants $A_{\rm dir}$ (in eV^3), C_{1s} (in eV^2) and φ_{1s} for double-ionization cross sections (equation (10)) of different isoelectronic sequences.

Sequence	Configuration	$A_{\rm dir}$	C_{1s}	φ_{1s}
He	$1s^2$	5.0	0	0
Li	$1s^22s$	12.0	0	0
Be	$1s^22s^2$	1.8	3.6	4.5
B	$1s^22s^22p^1$	10.0	3.6	5.0
C	$1s^22s^22p^2$	23.0	3.6	5.0
N	$1s^22s^22p^3$	43.0	3.6	5.0
O	$1s^22s^22p^4$	76.0	3.6	5.0
F	$1s^22s^22p^5$	133.0	3.6	5.0
Ne	$1s^22s^22p^6$	183.0	3.6	5.0

Table 3. First (I_1), second (I_2) potentials, the threshold energies $I_{\rm th}$ and binding energies I_{2p} and I_{2s} (all in eV) for Ar^{q+} ions, $q = 1$–7. The values of I_1 and I_2 are taken from tables (*Handbook of Chemistry and Physics* 2001), meanwhile I_{2s} and I_{2p} values were calculated by the GRASP code (Dyall *et al* 1989).

Ion	I_1	I_2	$I_{\rm th} = I_1 + I_2$	I_{2p}	I_{2s}
Ar^{0+}	15.759	27.629	43.388	249.25	327.04
Ar^{1+}	27.629	40.74	68.37	267.37	342.63
Ar^{2+}	40.74	59.81	100.55	280.21	359.79
Ar^{3+}	59.81	75.02	134.83	301.77	379.06
Ar^{4+}	75.02	91.007	166.03	320.46	399.92
Ar^{5+}	91.007	124.319	215.326	345.31	422.89
Ar^{6+}	124.319	143.456	267.775	373.41	447.09
Ar^{7+}	143.456	422.44	565.90	395.00	468.00

data have been obtained for C^{1+}, N^{2+}, O^{3+} and Ne^{5+} ions so far (Westermann *et al* 1999, Tinschert 1989).

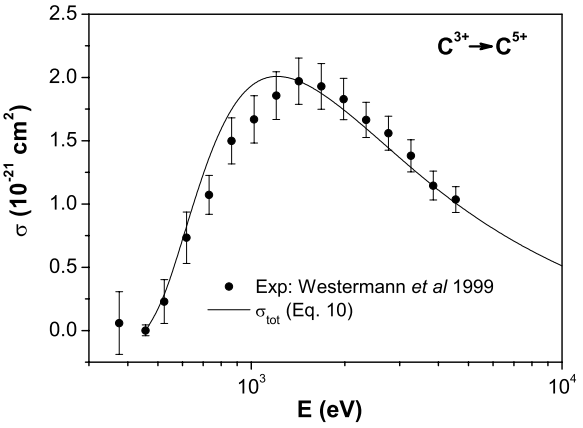

Figure 3. Double-ionization cross sections of Li-like C^{3+} ions. Solid circles, experimental data (Westermann *et al* 1999); solid curve, total cross section (equation (10)).

Table 4. Fitting constants $A_{\rm dir}$ (in eV^3), C_γ (in eV^2) and φ_γ for double ionization of argon atoms and ions.

Ions	Configuration	$A_{\rm dir}$	C_{2p}	φ_{2p}	C_{2s}	φ_{2s}
Ar^{0+}	$1s^22s^22p^63s^23p^6$	80.0	10.0	5.0	2.7	2.0
Ar^{1+}	$1s^22s^22p^63s^23p5$	67.0	11.0	5.0	2.7	2.0
Ar^{2+}	$1s^22s^22p^63s^23p^4$	40.0	13.0	5.0	2.7	2.0
Ar^{3+}	$1s^22s^22p^63s^23p^3$	33.0	13.0	5.0	2.7	2.0
Ar^{4+}	$1s^22s^22p^63s^23p^2$	27.0	15.0	5.0	2.7	2.0
Ar^{5+}	$1s^22s^22p^63s^23p^1$	20.0	15.0	5.0	2.7	2.0
Ar^{6+}	$1s^22s^22p^63s^2$	1.0	15.0	5.0	2.7	2.0
Ar^{7+}	$1s^22s^22p^63s^1$	2000.0	0.0	0.0	0.0	0.0

Table 5. Atomic parameters used for calculation of double ionization of Kr^{2+} ions. The binding energies were calculated using the GRASP code.

Shell γ	I_γ (eV)	C_γ (eV^2)	φ_γ	a_γ
$3d^{10}$	119.73	23.0	12.0	0.8
$3p^6$	246.5	8.0	5.0	0.6
$3s^2$	320.2	1.8	2.0	0.9

A comparison of experimental data for double-ionization cross sections of C^+ ions with the semiempirical formulae is given in figure 5. First of all, one can see that the experimental data obtained by the Louvain-la-Neuve and Giessen groups significantly differ from one another. Measurements by the Giessen group clearly show the profile of the first maximum due to direct double ionization, while the results of Zambra *et al* (1994) show not only lower values of the cross sections in the whole energy range but also significantly different energy dependence near the expected first maximum due to the direct double ionization. Such differences are noted for almost all data obtained by Zambra *et al*. The origin of the discrepancies is not clear.

We note here that the clear separation between the two maxima in the double-ionization cross sections together with other arguments mentioned above helped us to find suitable model

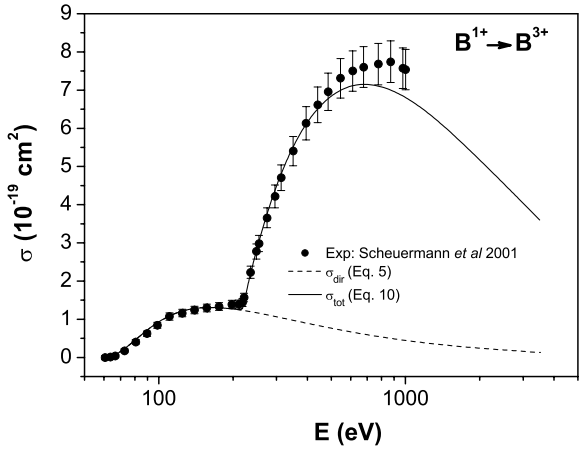

Figure 4. Double-ionization cross sections of Be-like B^+ ions. Solid circles: experimental data (Scheuermann *et al* 2001). Dashed curve, direct ionization cross section (equation (5)); solid curve, total cross section (equation (10)) with $a_{1s} = 1.0$.

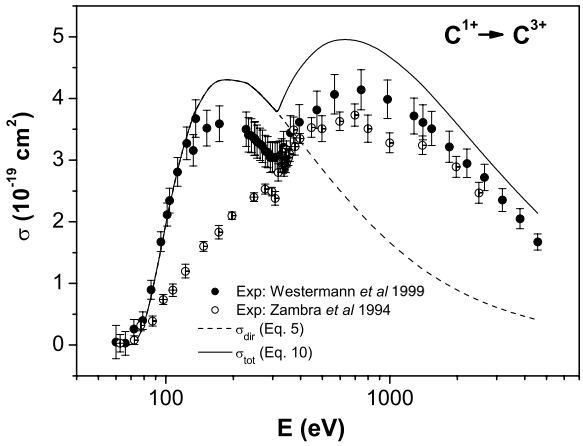

Figure 5. Double-ionization cross sections of B-like C^+ ions. Experimental data: solid circles—Westermann *et al* (1999), open circles—Zambra *et al* (1994). Dashed curve—direct ionization cross section (equation (5)), solid curve—total cross section (equation (10)) with $a_{1s} = 1.0$.

parameters for the description of direct double ionization. An additional argument for choosing the direct ionization cross section in the form (5) can also be inferred from the cross-section behaviour for single inner-shell ionization. The difference between experimental data for B-, C-, N-, F- and Ne-like ions, obtained by the Giessen group, and cross sections obtained from equation (5) coincide, within the experimental errors, with the 1s ionization cross sections calculated by using the ATOM-code (see above). Indeed, figure 6 shows as a typical example the 1s-shell ionization cross section for C^+ ions obtained from the experiment after subtraction of the model double-ionization cross section (equation (5)). The good agreement between the inferred experimental and calculated data for 1s-shell ionization of C^+ ions indicates the validity of equation (5) as an approach to direct double ionization.

In fact, using the procedure of subtracting $\sigma_{\rm dir}$ from experimental total double-ionization cross sections one can determine the 1s-ionization cross sections σ_{1s} of ions. Such inner-shell

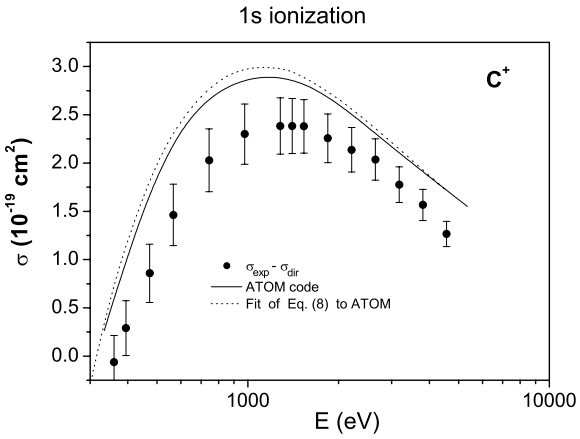

Figure 6. Single 1s-shell ionization cross sections for C^+ ions. Solid circles with error bars correspond to the experimental data shown in figure 5 (Westermann *et al* 1999) from which the direct double ionization contribution defined by equation (5) was subtracted. Solid curve, 1s-shell ionization cross section calculated by the ATOM code; dashed curve, least squares fit of equation (8). Both curves were plotted with $a_{1s} = 1.0$.

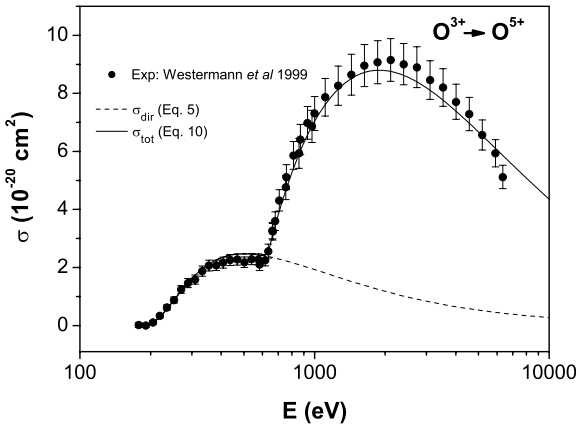

Figure 7. Double-ionization cross sections of B-like O^{3+} ions. Experimental data: solid circles (Westermann *et al* 1999). Dashed curve—direct ionization cross section (equation (5)); solid curve—total cross section (equation (10)) with $a_{1s} = 1.0$.

ionization cross sections have never been directly measured so far. In particular, from the present data for ions belonging to the Be-like to Ne-like isoelectronic sequences, σ_{1s} can be determined quite accurately by using the relation obtained from equation (12)

$$\sigma_{1s} = \frac{\sigma_{exp} - \sigma_{dir}}{a_{1s}}, \qquad E \geqslant I_{1s}, \tag{13}$$

where all quantities on the right-hand side of the equation are known.

Figure 7 shows a comparison of the experimental double-ionization cross section of O^{3+} ions with the semiempirical formulae (5) and (10). We note that good agreement is obtained using the same fitting parameters as for C^+ ions in figure 5.

Predicted double-ionization cross sections for neutral boron atoms and B-like Fe^{21+} ions are shown in figures 8 and 9, respectively. In both cases there is only one maximum but the

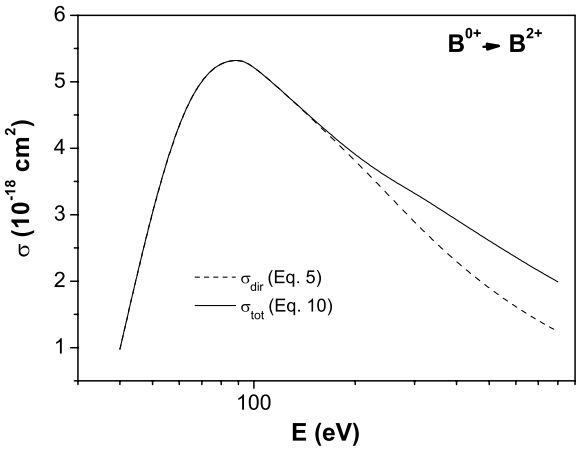

Figure 8. Predicted double-ionization cross section for neutral B atoms. Dashed curve, contribution from direct part (equation (5)); solid curve, total cross section (equation (10)) with $a_{1s} = 1.0$.

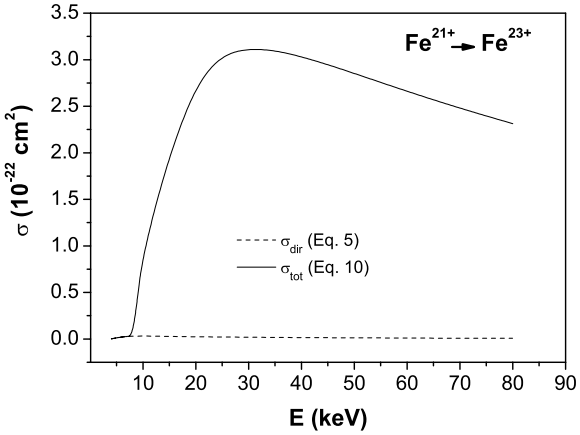

Figure 9. Predicted double-ionization cross section of B-like Fe^{21+} ions. Dashed curve, contribution from direct part (equation (5)); solid curve, total cross section (equation (10)) with $a_{1s} = 0.73$ (see table 6).

dominant mechanism is different in each case: in the first case the maximum is mainly due to direct ionization of two outermost electrons, while in the second case, the total cross section is caused dominantly by the single ionization of the 1s inner-shell electron. This feature can be explained within our model. Indeed, following equations (5) and (8), the maximum cross sections are

$$\sigma_{\rm dir}^{\rm max} \approx 1.7 \times 10^{-14}\,{\rm cm}^2\,\frac{A_{\rm dir}}{I_{\rm th}^3} \quad \text{at} \quad E_{\rm dir}^{\rm max} \approx 2.5 I_{\rm th} \tag{14}$$

$$\sigma_{\gamma}^{\rm max} \approx 7.6 \times 10^{-15}\,{\rm cm}^2\,\frac{C_\gamma}{I_\gamma^2}\,\frac{\sqrt{\varphi_\gamma}-1}{\varphi_\gamma\sqrt{\varphi_\gamma}+1} \quad \text{at} \quad E_{\gamma}^{\rm max} \approx I_\gamma\sqrt{\varphi_\gamma}, \tag{15}$$

where the energies $I_{\rm th}$ and I_γ are given in eV.

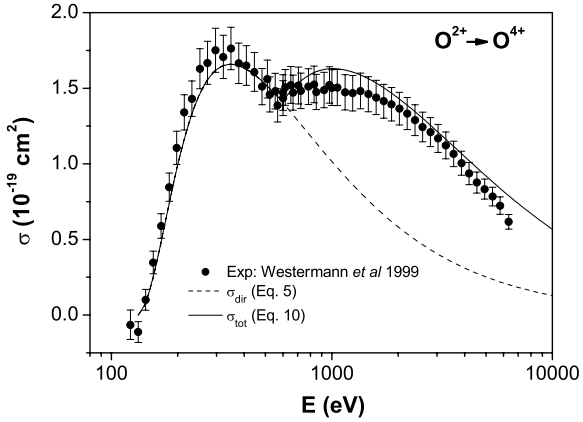

Figure 10. Double-ionization cross sections of C-like O^{2+} ions. Solid circles: experimental data (Westermann *et al* 1999). Dashed curve, direct ionization cross section (equation (5)); solid curve, total cross section (equation (10)) with $a_{1s} = 1.0$.

Taking the parameter $\varphi_{1s} \approx 5.0$ for all sequences considered, one gets the ratio of cross sections in their maxima

$$\frac{\sigma_{1s}^{max}}{\sigma_{dir}^{max}} \approx 0.45 \frac{C_{1s}}{A_{dir}} \frac{I_{th}^3}{I_{1s}^2}. \tag{16}$$

Using the data in tables 1 and 2 one obtains for B-like ions:

$$\frac{I_{th}^3}{I_{1s}^2} \approx 1.2(q+1)^2 \,\text{eV}, \tag{17}$$

and

$$\frac{\sigma_{1s}^{max}}{\sigma_{dir}^{max}} \approx 0.2(q+1)^2. \tag{18}$$

This interesting $(q + 1)^2$-dependence in equations (17) and (18) shows that for neutral targets ($q = 0$), the ratio $\sigma_{1s}^{max}/\sigma_{dir}^{max} \approx 0.2$, and, thus, the contribution of the direct ionization is dominant. Indeed, only one maximum created by the direct simultaneous ionization of two electrons is observed. For low-charged ions ($q = 1$–2, i.e., for C^+ and N^{2+}), $\sigma_{1s}^{max}/\sigma_{dir}^{max} \approx 1$, and the two maxima are of comparable size. For highly charged ions ($q \gg 1$), the contribution from direct ionization is very small, and double ionization occurs mainly due to the single ionization of one 1s electron followed by a subsequent Auger transition.

3.5. C-like ions

In the case of C-like ions, experimental data are available only for N^{1+} and O^{2+} ions. As an example, we present the cross sections for O^{2+} ions in figure 10. Similar to the case of B-like ions considered above, there are two maxima of the cross section due to the direct and indirect contributions which are of comparable size.

3.6. N-like ions

In this case, experimental data are available only for double ionization of O^+ ions. A comparison with our calculations is given in figure 11. Here, direct double ionization is clearly dominant over the 1s-shell ionization. Note that the data from two experimental groups show quite different features. The present analysis agrees with those from the experimental cross sections obtained in Giessen.

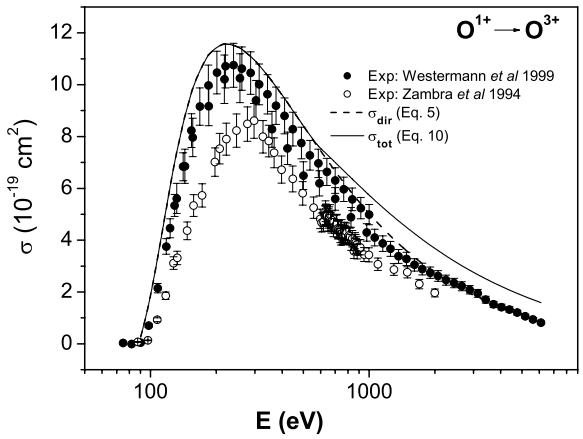

Figure 11. Double-ionization cross sections of N-like O^+ ions. Experiment: solid circles—Westermann *et al* (1999), open circles Zambra *et al* (1994). Dashed curve—direct ionization cross section (equation (5)), solid curve—total cross section (equation (10)) with $a_{1s} = 1.0$.

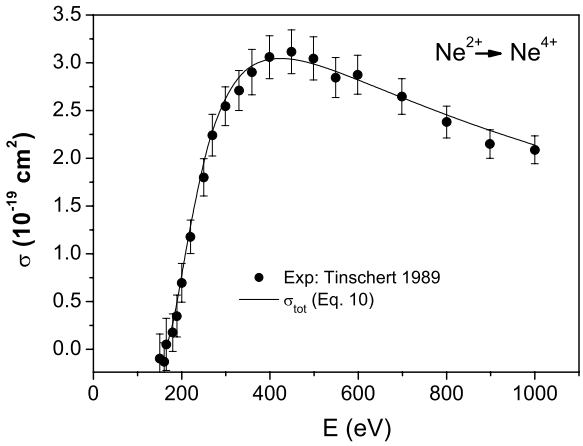

Figure 12. Double-ionization cross sections of O-like Ne^{2+} ions. Experiment: solid circles—Tinschert *et al* (1989). Solid curve—total cross section (equation (10)) with $a_{1s} = 1.0$.

3.7. O-like ions

Experimental data are available for double ionization of O atoms (Zipf 1985, Thompson *et al* 1995) and Ne^{2+} ions (Tinschert 1989). The double-ionization cross sections for Ne^{2+} ions are shown in figure 12. Since the binding energy of a 1s-electron is quite large ($I_{1s} = 926.38$ eV), the influence of K-shell ionization is almost not seen in the experimental cross sections which were measured below 1000 eV.

3.8. F-like ions

As for F-like ions, experimental data are available for Ne^+ and Al^{4+} ions (Tinschert 1989, Steidl *et al* 1999). A comparison of the data for Ne^+ ions with the present calculations is

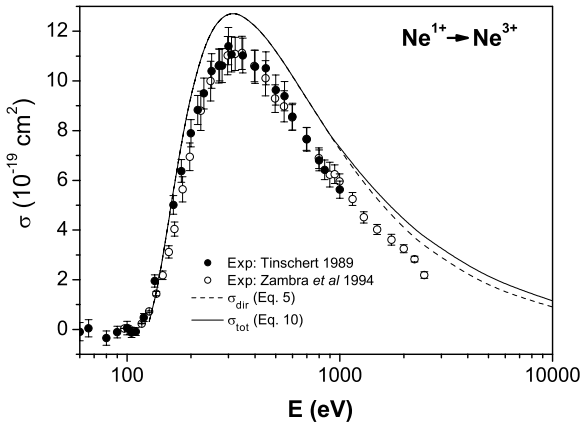

Figure 13. Double-ionization cross sections of F-like Ne^+ ions. Experiment: solid circles—Tinschert (1989), open circles—Zambra *et al* (1994). Dashed curve—direct ionization cross section (equation (5)), solid curve—total cross section (equation (10)) with $a_{1s} = 1.0$.

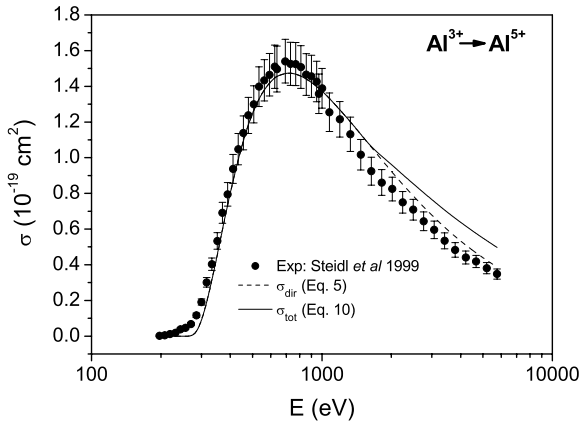

Figure 14. Double-ionization cross sections of Ne-like Al^{3+} ions. Experiment: solid circles—Steidl *et al* (1999). Dashed curve—direct ionization cross section (equation (5)), solid curve—total cross section (equation (10)) with $a_{1s} = 1.0$.

shown in figure 13. Similar to the case of O-like ions, the contribution from single-ionization of a 1s-electron is very small since, according to equation (18),

$$\frac{\sigma_{1s}^{max}}{\sigma_{dir}^{max}} \approx 0.45 \frac{C_{1s}}{A_{dir}} \frac{I_{th}^3}{I_{1s}^2} \approx 0.02. \tag{19}$$

3.9. Ne-like ions

Experimental data are available for Ne, Na^+ and Al^{3+} ions (Schram *et al* 1966, Hirayama *et al* 1986, Steidl *et al* 1999, van der Wiel *et al* 1969). The data on Al^{3+} are presented in figure 14. Again, the contribution from ionization of a 1s-electron to the total double-ionization cross

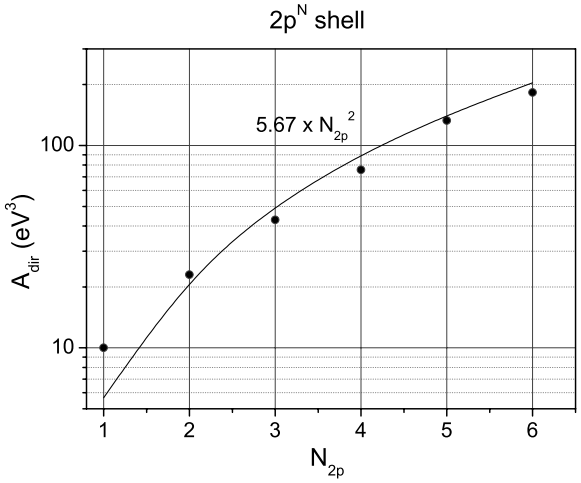

Figure 15. Dependence of the fitting parameter $A_{\rm dir}$ on the number of equivalent electrons $N_{2\rm p}$ for target ions with the outer-shell configuration $2p^N$: solid circles—data obtained from experiment, solid curve—average curve described by the quadratic function $A_{\rm dir} = 5.67\ N_{2\rm p}^2$ (present work).

section for Al^{3+} ions is quite small:

$$\frac{\sigma_{1\rm s}^{\rm max}}{\sigma_{\rm dir}^{\rm max}} \approx 0.067. \tag{20}$$

We can now summarize our findings for double ionization of He-like through Ne-like ions. The fitting parameters $A_{\rm dir}$, $C_{1\rm s}$ and $\varphi_{1\rm s}$ for isoelectronic sequences considered above are summarized in table 2. The constants $A_{\rm dir}$ are also plotted in figure 15 as a function of the number of equivalent electrons $N_{2\rm p}$ in the outer 2p shell of these ions. This dependence can be approximately described by a smooth quadratic function $A_{\rm dir} = 5.67\ N_{2\rm p}^2$, which shows a smooth dependence on the number of 2p-electrons.

3.10. Double ionization of Ar^{q+} ions with $q = 1$–7

Double ionization of heavier ions such as Ar^{q+} with $q = 1$–7 was also considered in this work. In these ions, the contribution of the 2s and 2p inner-shell electrons has to be taken into account. (Ionization of the 1s-shell is not possible at the present energies.) The threshold energies for 2s- and 2p-shell ionizations were taken from the tables (*Handbook of Chemistry and Physics* 2001) or were calculated using the GRASP code (Dyall *et al* 1989); the corresponding values are given in table 3. The fitting parameters found for these ions are given in table 4. The difference between Ar ions and the ions considered in the previous sections is that for Ar ions one has to take into account two groups of electrons, $2s^2$ and $2p^6$, which make our treatment more complicated.

In figure 16, we summarize the experimental data for double ionization of Ar atoms, $q = 0$ (Syage 1991) and Ar^{q+} ions with $q = 1$–7 (Müller *et al* 1985a) which are compared with the semiempirical formula (10). In some cases (e.g., Ar^{2+}, Ar^{5+}) the ionization energies were slightly changed (about 10%) to higher/lower values just to fit the calculated cross sections to experiment. We also note that for highly charged argon ions ($q = 6$, 7) the fitting parameters have a large uncertainty because the number of experimental points is very small and the cross sections have relatively large error bars.

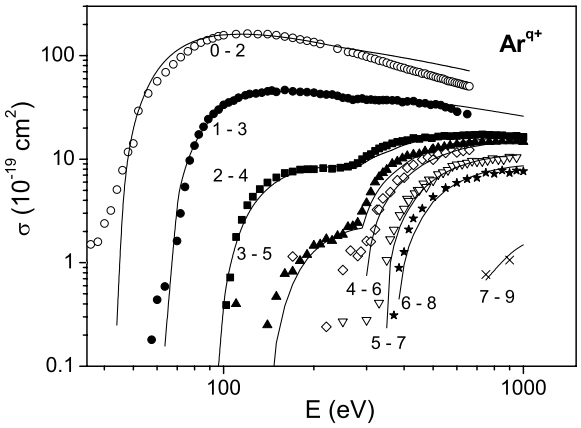

Figure 16. Double-ionization cross sections of Ar atoms ($q = 0$) and Ar^{q+} ions ($q = 1$–7). Experiment: open circles—double-ionization cross section of neutral Ar (Syage 1991), other symbols—double ionization of Ar ions (Müller *et al* 1985a). Solid curves—total cross sections, (equation (10)) with fitting parameters listed in table 4.

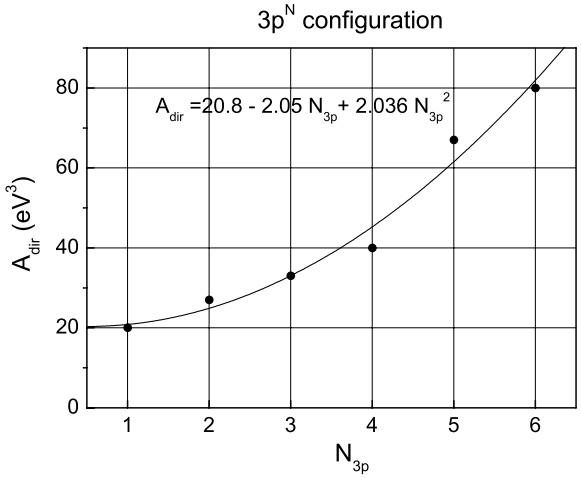

Figure 17. Dependence of the fitting parameter $A_{\rm dir}$ on the number of equivalent electrons $N_{3\rm p}$ for target ions with the outer-shell configuration $3p^N$: solid circles—data obtained from experiment, solid curve—average curve described by the quadratic function $A_{\rm dir} = 20.8–2.05\,N_{3\rm p} + 2.036\,N_{3\rm p}{}^2$.

In figure 17 we reproduce the dependence of the fitting parameter $A_{\rm dir}$ for direct double ionization as a function of the number of equivalent electrons $N_{3\rm p}$ for Ar ions with $3p^N$ configurations of the outer-shell electrons. Similar to $2p^N$ configurations (figure 15), $A_{\rm dir}$ is also a smooth quadratic function of $N_{3\rm p}$.

3.11. Kr^{q+} ions, $q = 1$–4

Double ionization of heavy Kr^{q+} ions with $q = 1$–4 was also considered to test our semiempirical formulae. We found that it is possible, in principle, to estimate the cross sections but then one has to know quite exactly the branching ratios of decays subsequent to inner-shell ionization. For these ions the binding energy of the inner-shell 3d-electrons is quite

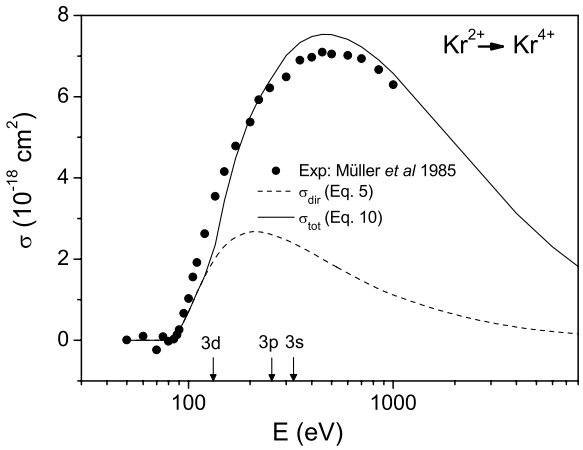

Figure 18. Double-ionization cross sections of Kr^{2+} ions. Experiment: solid circles—Müller *et al* (1985a, 1985b). Dashed curve—direct ionization cross section (equation (5)), dotted curve—the total cross section (equation (10)) with $A_{\rm dir} = 83.3$, energies $I_{\rm th} = 80$ eV, $I_{3\rm d} = 119.73$ eV, $I_{3\rm p} = 246.5$ eV, $I_{3\rm s} = 320.2$ eV and branching ratios $a_{3\rm d} = 0.8$, $a_{3\rm p} = 0.6$, $a_{3\rm s} = 0.9$ which were found by fitting the experimental data. Arrows indicate the threshold energies for inner-shell ionization.

close to the threshold energy of the double-electron ionization which makes an interpretation of the experimental data difficult. A typical example of the double-ionization cross sections of Kr^{2+} is shown in figure 18 in comparison with experimental data. Though fairly crude, the present model can generally reproduce the observed data even for such complicated many-electron ions as Kr^{2+} ions.

4. Fluorescence yields $\omega_{\rm K}$ for a single 1s-shell vacancy

In calculations of inner-shell contributions to double ionization of light ions the branching ratios a_γ defined by equation (4) can be safely assumed to be unity because for low-charged ions the autoionization rates $A_{\rm a}$ have a weak dependence on the ion charge and are much larger than the radiative decay rates $A_{\rm r}$: $A_{\rm a} \gg A_{\rm r}$. With the ion charge increasing, the $A_{\rm r}$ values increase approximately as $A_{\rm r} \sim q^4$ and become comparable and then even much larger than $A_{\rm a}$ leading to a decrease of the branching ratio a_γ.

In order to obtain the branching ratios $a_{1\rm s}$ for ions from Li-like to Ne-like isoelectronic sequences, including heavy ions, we calculated the fluorescence yield $\omega_{\rm K} = 1 - a_{1\rm s}$ for these ions up to the nuclear charge $Z = 26$ (see table 6). Calculations of the fluorescence yields $\omega_{\rm K}$ were performed using the relativistic, multiconfigurational atomic package FAC (flexible atomic calculations) described by Gu (2003). Within FAC, the bound-state wavefunctions are calculated using a fully relativistic configuration–interaction method and the jj-coupling scheme. The radiative decay rates are calculated using the electric dipole approximation with only E1 transitions included. The autoionization rates are calculated using the distorted wave approximation.

The statistically averaged $\omega_{\rm K}$-values are given in table 6:

$$\omega_{\rm K} = \frac{1}{\sum_i (2J_i + 1)} \sum_i (2J_i + 1) \frac{A_{\rm r}^{(i)}}{A_{\rm a}^{(i)} + A_{\rm r}^{(i)}}, \tag{21}$$

where the index i denotes a specific initial state with the total angular momentum J_i.

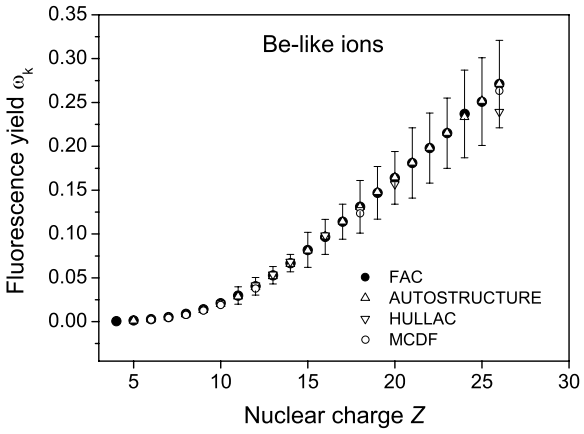

Figure 19. Comparison of calculated fluorescence yields ω_K for Be-like ions (configuration $1s^12s^22p$) as a function of the ion nuclear charge Z: FAC—present work; other data are from the work by Gorczyca *et al* (2003). The computer codes used in calculations are indicated in the figure.

Table 6. Calculated fluorescence yields ω_K for ions from Li-like to Ne-like isoelectronic sequences using the FAC code (present work). The accuracy is estimated to be about 20%.

Nuclear charge Z	Li-like	Be-like	B-like	C-like	N-like	O-like	F-like	Ne-like
3	5.2×10^{-5}	–	–	–	–	–	–	–
4	1.45×10^{-4}	5.73×10^{-4}	–	–	–	–	–	–
5	3.2×10^{-4}	0.001 36	0.002 51	–	–	–	–	–
6	6.4×10^{-4}	0.001 49	0.003 55	0.003 74	–	–	–	–
7	0.00114	0.005 18	0.006 44	0.0074	0.0064	–	–	–
8	0.001 88	0.008 77	0.0108	0.012	0.0099	0.0101	–	–
9	0.002 94	0.0141	0.017	0.0186	0.0147	0.0145	0.0144	–
10	0.004 37	0.021	0.0253	0.0275	0.0212	0.0204	0.0197	0.0201
11	0.006 26	0.0298	0.0359	0.0387	0.0297	0.028	0.0266	0.0269
12	0.0087	0.0404	0.0488	0.0427	0.0403	0.0377	0.0352	0.0355
13	0.0117	0.0529	0.0638	0.0666	0.0535	0.0496	0.0459	0.046
14	0.0154	0.0668	0.0808	0.083	0.0692	0.0643	0.0588	0.0588
15	0.0198	0.0819	0.0994	0.102	0.0876	0.0808	0.0742	0.074
16	0.025	0.0968	0.119	0.123	0.108	0.1	0.0921	0.0916
17	0.031	0.114	0.142	0.147	0.131	0.122	0.113	0.112
18	0.0378	0.131	0.165	0.174	0.157	0.147	0.136	0.134
19	0.0456	0.147	0.19	0.203	0.186	0.174	0.161	0.16
20	0.0541	0.164	0.215	0.232	0.216	0.204	0.189	0.187
21	0.067	0.181	0.241	0.263	0.248	0.235	0.219	0.216
22	0.0739	0.198	0.28	0.296	0.282	0.267	0.25	0.247
23	0.0855	0.215	0.325	0.328	0.319	0.302	0.283	0.28
24	0.0968	0.237	0.353	0.362	0.354	0.337	0.317	0.313
25	0.109	0.251	0.401	0.395	0.39	0.374	0.352	0.348
26	0.123	0.271	0.432	0.428	0.435	0.408	0.387	0.382

The calculated fluorescence yields ω_K for ions from the Li-like to Ne-like isoelectronic sequences are given in table 6. The first value in each column corresponds to the fluorescence yield of the inner-shell excited neutral atom, e.g., the value of $\omega_K = 0.002\,51$ for $Z = 5$ in

B-like systems is for the neutral $[B(1s^1 2s^2 2p^2)]^{**}$ atom. All other values are for positive ions. For example, for Be-like Fe ions, we find $\omega_K = 0.271$ which corresponds to the fluorescence yield of the excited $Fe^{22+}(1s^1 2s^2 2p^1)$ ion.

One can see from table 6 that for ions with $Z < 18$, the ω_K values are quite small with $\omega_K \ll 1$. Thus, the branching ratios are close to unity, i.e., $a_{1s} \approx 1$. For higher Z with $Z > 18$, the fluorescence yields increase and the branching ratios a_{1s} decrease. For example, the fluorescence yield ω_K and the branching ratio a_{1s} for ions from the B-like sequence are: for $Z = 18$, $\omega_K = 0.165$, $a_{1s} = 0.835$ and for $Z = 26$, $\omega_K = 0.432$, $a_{1s} = 0.568$.

We note that the calculated ω_K values given in table 6 are in good agreement (within 20%) with available accurate calculations for neutral atoms (McGuire 1969, Krause 1979) and Be-like and F-like ions (Gorczyca *et al* 2003). Typical behaviour of the fluorescence yield ω_K for the Be-like system is shown in figure 19 where the present calculations (solid circles with error bars) are compared with calculations by Gorczyca *et al* (2003) using different codes: AUTOSTRUCTURE, HULLAC and MCDF (see Gorczyca *et al* (2003) for details).

5. Conclusions

A new semiempirical formula was obtained to describe the electron-impact *double*-ionization cross sections σ_2 of light atoms and ions. It consists of two terms representing the two processes which predominantly contribute to the cross sections. The first term describes direct simultaneous ionization of two of the outermost electrons. The cross section scales as $\sigma_{dir} \sim I_{th}^{-3}$ when plotted as a function of the scaled electron energy E/I_{th} with I_{th} being the threshold energy. Most probably, this dependence is a result of the correlation effects relevant to double ionization.

Another term was obtained for single ionization of a 1s electron from atoms and positive ions on the basis of quantum mechanical calculations combined with a least-squares fit of the theoretical data. Together with calculated branching ratios a_{1s}, our formula describes ionization–autoionization cross sections contributing to double ionization. A combination of the two formulae allows one to reproduce available experimental data for light ions from He-like to Ne-like isoelectronic sequences with an accuracy of 20–30% and to predict double-ionization cross sections of positive ions with the nuclear charge $Z < 25$ in the energy range of $E < 50\, I_{th}$. For heavier ions or/and higher energies, one has to take into account the Bethe logarithmic term in the high-energy parts of the cross sections and relativistic effects in the wavefunctions and interaction potentials.

Acknowledgments

The authors are grateful to H Bräuning and R Trassl for valuable discussions and to Z Harman and M F Gu for their advice on the use of the computer codes GRASP and FAC. One of the authors (VPS) is grateful to DFG for financial support under grant 436 RUS 17/89/04. This work was also supported in part by the Russian grant RFBR no 04-02-16309 and INTAS grant no 03-54-3604.

References

Andersen L H, Hvelplund P, Knudsen H, Møller S P and Sørensen A H 1987 *Phys. Rev.* A **36** 3612

Bélenger C, Defrance P, Salzborn E, Shevelko V P, Tawara H and Uskov D B 1997 *J. Phys. B: At. Mol. Opt. Phys.* **30** 2667

Deutsch H, Becker K and Märk T D 1996 *J. Phys. B: At. Mol. Opt. Phys.* **29** L497

Duponchelle M, Khoeilid M, Oualim E M, Zhang H and Defrance P 1997 *J. Phys. B: At. Mol. Opt. Phys.* **30** 729
Dyall K D, Grant I P, Johnson C D, Parpia F A and Plummer E P 1989 *Comput. Phys. Commun.* **55** 425
Fisher V, Ralchenko Yu, Godrish A, Fisher D and Maron Y 1995 *J. Phys. B: At. Mol. Opt. Phys.* **28** 3027
Gorczyca T W, Kodituwakki C N, Korista K T, Zatsarinny O, Badnell N R, Chen M H and Savin D W 2003 *Astrophys. J.* **592** 636
Gu M F 2003 *Astrophys. J.* **582** 1241
Handbook of Chemistry and Physics 2000–2001 81st edn, ed D R Lide (Boca Raton, LA: CRC Press)
Hirayama T, Oda K, Morikawa Y, Sano T, Ikezaki Y, Takayanagi T, Wakiya K and Suzuki H 1986 *J. Phys. Soc. Japan* **55** 1411
Hofmann G, Müller A, Tinschert K and Salzborn E 1990 *Z. Phys.* D **16** 113
Krause M O 1979 *J. Phys. Chem. Ref. Data* **8** 307
Lotz W 1970 *J. Opt. Soc. Am.* **60** 206
McGuire E J 1969 *Phys. Rev.* **185** 1
McGuire J H 1992 *Adv. At. Mol. Opt. Phys.* **29** 217
Müller A, Tinschert K, Achenbach C, Becker R and Salzborn E 1985a *J. Phys. B: At. Mol. Phys.* **18** 3011
Müller A, Tinschert K, Achenbach C, Salzborn E and Becker R 1985b *Nucl. Instrum. Methods.* B **10/11** 204
Müller A 1991 *Physics of Ion Impact Phenomena* ed D Mathur (*Springer Ser. Chem. Phys.* vol 54) (Berlin: Springer)
Müller A 2002 Experimental data for electron–ion collisions *Atomic and Molecular Data and Their Applications (3rd Int. Conf. on Atomic Data and Their Applications ICAMDATA (Gatlinburg TN 24–27 April 2002)* (*AIP* vol 636) ed D R Schulz, P S Krstić and F Ownby (New York: Melville)
Peart B and Dolder K T 1969 *J. Phys. B: At. Mol. Phys.* **2** 1169
Scheuermann F, Jacobi J, Salzborn E and Müller A 2001 *Giessen* unpublished
Schram B L, Boerboom A J and Kistemaker H 1966 *Physica* **32** 185
Shah M B, Elliot D S, McCallion P and Gilbody H B 1988 *J. Phys. B: At. Mol. Opt. Phys.* **21** 2756
Shevelko V P and Vainshtein L A 1993 *Atomic Physics for Hot Plasmas* (Bristol: Institute of Physics Publishing)
Shevelko V P and Tawara H 1998 *Atomic Multielectron Processes* (Berlin: Springer)
Steidl M, Aichele K, Hartenfeller U, Hathiramani D, Pindzola M S, Scheuermann F, Westermann M and Salzborn E 1999 *Abstractbook of 21st Int. Conf. on the Physics of Electronic and Atomic Collisions (Sendai, Japan, 22–27 July 1999)* ed Y Itikawa, K Okuno, H Tanaka, A Yagishita and M Matsuzawa (Abstracts of Contributed Papers) p 362
Syage J A 1991 *J. Phys. B: At. Mol. Opt. Phys.* **24** L527
Tawara H and Kato T 1987 *At. Data Nucl. Data Tables* **36** 167
Tawara H and Kato M 1999 *NIFS-DATA-51* National Institute for Fusion Science, Toki, Japan
Thompson W R, Shah M B and Gilbody H B 1995 *J. Phys. B: At. Mol. Opt. Phys.* **28** 1321
Tinschert K, Müller A, Phaneuf R A, Hofmann G and Salzborn E 1989 *J. Phys. B: At. Mol. Opt. Phys.* **22** 1241
Tinschert K 1989 *PhD Thesis* Giessen University
van der Wiel M J, El-Sherbeni T M and Vriens L 1969 *Physica* **42** 411
Wannier G H 1953 *Phys. Rev.* **90** 817
Westermann M, Scheuermann F, Aichele K, Hathiramani D, Steidl M and Salzborn E 1999 *Phys. Scr.* T **80** 285
Zambra M, Belić D, Defrance P and Yu D J 1994 *J. Phys. B: At. Mol. Opt. Phys.* **27** 2383
Zipf E C 1985 *Planet. Space Sci.* **33** 1303